

## Classification of contralateral and ipsilateral finger movements for electrocorticographic brain-computer interfaces

REINHOLD SCHERER, PH.D.,<sup>1</sup> STAVROS P. ZANOS, M.D.,<sup>2</sup> KAI J. MILLER, PH.D.,<sup>3</sup>  
RAJESH P. N. RAO, PH.D.,<sup>1</sup> AND JEFFREY G. OJEMANN, M.D.<sup>4</sup>

*Departments of <sup>1</sup>Computer Science and Engineering, <sup>2</sup>Physiology and Biophysics, <sup>3</sup>Physics, and <sup>4</sup>Neurological Surgery, University of Washington, Seattle, Washington*

Electrocorticography (ECoG) offers a powerful and versatile platform for developing brain-computer interfaces; it avoids the risks of brain-invasive methods such as intracortical implants while providing significantly higher signal-to-noise ratio than noninvasive techniques such as electroencephalography. The authors demonstrate that both contra- and ipsilateral finger movements can be discriminated from ECoG signals recorded from a single brain hemisphere. The ECoG activation patterns over sensorimotor areas for contra- and ipsilateral movements were found to overlap to a large degree in the recorded hemisphere. Ipsilateral movements, however, produced less pronounced activity compared with contralateral movements. The authors also found that single-trial classification of movements could be improved by selecting patient-specific frequency components in high-frequency bands (> 50 Hz). Their discovery that ipsilateral hand movements can be discriminated from ECoG signals from a single hemisphere has important implications for neurorehabilitation, suggesting in particular the possibility of regaining ipsilateral movement control using signals from an intact hemisphere after damage to the other hemisphere. (DOI: 10.3171/2009.4.FOCUS0981)

**KEY WORDS** • electrocorticography • brain-machine interface •  
machine learning • neuro-rehabilitation • learning vector quantization •  
motor control • classification

THE 2 dominant paradigms for brain-computer interfacing today rely on noninvasive recording from the scalp (known as electroencephalography or EEG)<sup>3,38</sup> and invasive techniques based on intracortical implants that are placed inside the brain.<sup>7,15</sup> Although EEG-based systems are cheap and relatively easy to build, the EEG signals themselves are extremely noisy, thereby limiting the bandwidth of control signals that can be reliably extracted. On the other hand, the signals recorded using intracortical implants are much stronger, typically allowing one to record the individual spiking activities of several 10s of neurons. However, being invasive, intracortical implants pose serious health risks and have only been used in a few cases in humans. Noninvasive techniques such as fMR imaging do not have the temporal resolution needed by BCIs: because fMR imaging measures changes in blood oxygenation levels,

events are temporally smeared by the vascular response.

Electrocorticography overcomes many of the above problems. In ECoG electrical activity is recorded using an array of electrodes placed on the surface of the brain. It is typically performed in patients who are being monitored prior to epilepsy surgery. Because ECoG electrodes do not penetrate the brain surface, they are not as invasive as intracortical implants. Additionally, ECoG allows electrical signals from several different brain areas to be recorded while at the same time providing temporal resolution in the millisecond range. Electrocorticography can provide higher spatial resolution and signal-to-noise ratio than EEG<sup>17</sup> and higher temporal resolution than fMR imaging. It also minimizes the effects of muscle and movement artifacts commonly seen in EEG. Because of these factors, we and others have proposed ECoG as an ideal target for brain-machine computer (BCI) applications<sup>14,16,18,21,28,30,31,33</sup> and have shown how advanced mathematical methods allow for fast and accurate isolation of BCI control signals without requiring prior knowledge of salient signal features: particular electrodes and frequencies for BCI control do not need to be determined ahead

*Abbreviations used in this paper:* BCI = brain-computer interface; DSLVQ = distinction-sensitive LVQ; ECoG = electrocorticography; EEG = electroencephalography; EMG = electromyography; fMR = functional MR; LVQ = learning vector quantization.

of time but can be automatically tuned to the individual's ECoG signals.<sup>35,36</sup>

The ability to decode information about movements from ECoG has been well demonstrated.<sup>6,8,9,11,13,14,19,22,25,27</sup> One concern is whether these potential control signals for BCI are still present in an individual with a damaged brain.<sup>13</sup> This concern can be addressed by the identification of signals that are likely to be preserved after neurological damage. For example, loss of subcortical function, as with an internal capsule stroke, is likely to leave ipsilateral motor function relatively preserved compared with contralateral function. The study of cortical signals during ipsilateral movements has received attention recently.<sup>32,37,40</sup>

In this article, we report results from 2 patients who performed movement of different digits (thumb and index finger) in both the ipsilateral and contralateral hand. We found oscillatory components in the ECoG signal that accurately predicted the movement of a specific finger and also which side moved (ipsilateral vs contralateral). The identification of individual finger movements from ECoG may open the door to eventual BCI control of a prosthetic hand. Further, the ability to classify individual movements of *ipsilateral* fingers may prove to be extremely useful for neurorehabilitation.

## Methods

### *Patients and Data Acquisition*

The study participants were 2 neurosurgical patients with intractable epilepsy. Both underwent temporary placement of a subdural electrode array to localize the epileptic seizure focus and map brain function prior to surgical resection. Electrode placement was determined by clinical considerations, with the necessity and location of the electrodes determined by the interdisciplinary conference of the Regional Epilepsy Center, Harborview Medical Center, University of Washington. The patients gave informed consent prior to participation in a manner approved by the Human Studies Division (Institutional Review Board) of the University of Washington.

**Patient 1.** This 27-year-old left-handed man, with normal examination results, had previously undergone resection of dysplasia in the inferior portion of anterior parietal cortex. His seizures were focal motor and a higher density array was implanted around the central sulcus. The focus was at the anterior-inferior aspect of motor cortex and frontal operculum. The subdural array comprised 32 "regular" clinical ECoG electrodes (0.4-cm diameter), at 1-cm horizontal and vertical interelectrode distance, interleaved with 21 smaller ECoG electrodes (0.2-cm diameter), at 1-cm horizontal and 0.7-cm vertical interelectrode distance (Integra LifeSciences Corp.). Six surface EMG electrodes were used on the anterior surface of the left shoulder, flexor and extensor surfaces of the left forearm, and back of the left hand to monitor the seizures. Initial maps of motor function were previously reported for this patient.<sup>40</sup>

**Patient 2.** This 24-year-old right-handed man, with

a history of left frontal contusion following closed head injury, presented with partial seizures. He underwent a frontal electrode array placement with the posterior aspect of the array (Ad-Tech Medical Instrument Corp.) covering the central sulcus. The results of his motor function examination were normal. The focus was left anterior and superior frontal, away from the motor cortex.

Electrocorticography and EMG signals were recorded on a Synamp2 amplifier (Compumedics Neuroscan) at a sampling rate of 2000 samples per second and bandpass filtered between 1 and 500 Hz. The position of each finger was registered through a 5-degrees of freedom data glove device (Fifth Dimension Technologies, Inc.).

### *Experimental Paradigm*

The patients were told to perform a simple cue-guided repetitive motion task of left or right thumb or index finger movements. Three-second-long visual cues for whole hand, thumb, or index finger were randomly interleaved and separated by 2-second rest intervals. The cues were delivered visually on a 10 × 10-cm presentation window at a distance of 70 cm from the subject, using the BCI2000 software.<sup>29</sup> In total there were at least 30 cue presentations per type of visual cue, for both ipsilateral and contralateral tasks. The results in this paper focus on finger movements; data from whole hand movements were excluded from this study.

### *Data Analysis*

After the ECoG signal was downsampled to 500 samples per second, it was visually inspected for the presence of artifacts and noisy segments, which were removed. It was then re-referenced with respect to the common average (the arithmetically average signal of all electrodes was subtracted from each electrode).

**Time-Frequency Maps.** To get a general view of patient-specific power modulation patterns in relation to movement, time-frequency maps were calculated.<sup>10,12</sup> These maps are time-frequency plots that display significant power decrease or increase in predefined frequency bands.<sup>24</sup> Trials of 5 seconds' duration (1 second before and 4 seconds after cue onset) were used to calculate the time-frequency maps. To remove the influence of event-related potentials, the intertrial variance method was applied.<sup>10</sup> The baseline activity (that is, the reference value that was used to calculate relative power changes) was defined from  $t = -0.75$  seconds to  $t = -0.25$  seconds. Frequency bands 2 Hz wide with 1 Hz overlap and ranging from 6 to 125 Hz were calculated. Details about the calculation of these maps have been previously reported.<sup>10,12</sup>

**Feature Selection and Single-Trial Classification.** Machine learning and pattern recognition refer to mathematical algorithms that allow automatic identification of statistical patterns in data. This is particularly useful for signal classification that may ultimately be used for BCI applications. For example, a machine learning classifier can be used learn to map specific patterns for ECoG activity to either middle or index finger movement by training the classifier on an initial set of data where the mapping is

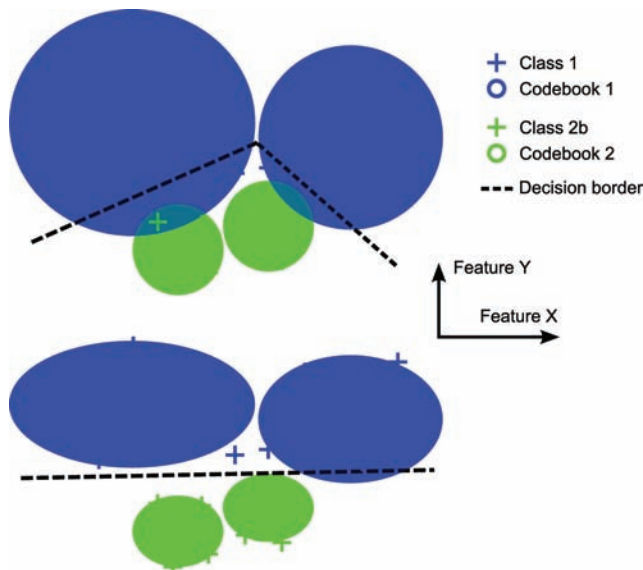


FIG. 1. Schematic illustration of the DSLVQ principle. Given is a 2-class classification problem and observations for Features X and Y. Each class is represented by a cluster center (codebook) comprising 2 clusters. The *upper plot* illustrates the clustering of the training data. The resulting decision border is not optimal for classification. By weighting the influence of features, the decision border can be adjusted and misclassification reduced. In this case Feature Y is relevant for classification.

known (movement was elicited by a cue-based paradigm). This trained classifier can subsequently be used to classify new ECoG activity into one of the two movement classes, which can then be converted to an output control signal for a BCI device.

To identify the structure of oscillatory components during different movement tasks, the distinction-sensitive learning vector quantization (DSLVQ) method<sup>26</sup> was applied to the data. Previously DSLVQ was successful applied to ECoG signals to study spectral components in the low frequency range (8–40 Hz).<sup>31</sup> Distinction-sensitive LVQ approximates the distribution of the analyzed data by forming clusters; labeled training data are represented by a set of reference points (a codebook) and a distance function. Classification is achieved by assigning new unlabeled data samples to the label of its closest codebook. (Figure 1 shows an example with 2 classes.) Because of the resulting decomposition of the feature space into cells, the resulting decision border is composed of multiple linear pieces. During training, these pieces are analyzed independently and their position is adjusted. Distinction-sensitive LVQ makes adjustments by weighting the influence of individual features—the influence of features that contribute to classification is increased, while that of features that lead to a misclassification is reduced (Fig. 1). The main advantage of DSLVQ is that it does not require expertise or any a priori knowledge about the distribution of the data. Because the training is based on data representation rather than on error minimization, even for high-dimensional feature problems with a low number of samples, some generalization can be found.

The spectral components used by DSLVQ were computed by bandpass filtering the signal from single trials,

with a fourth-order Butterworth filter, squaring and averaging the samples over 1-second intervals (moving average). A 1-second interval was selected because in Patient 1, the average duration for a single movement of a finger was about 1 second. Individual DSLVQ analyses were computed from features extracted from 9 overlapping time intervals of 1 second's length and a time lag of 0.5 seconds (starting with cue onset at  $t = 0.0$  seconds). For each time interval, 32 logarithmic band power features between 6 and 120 Hz (6–16 Hz, bandwidth 2 Hz, no overlap; 16–40 Hz, bandwidth 4 Hz, overlap 2 Hz; 40–120 Hz, bandwidth 10 Hz, overlap 5 Hz) were computed. To stabilize the variance of spectral components, a logarithmic transformation was performed prior to DSLVQ analysis.<sup>2</sup> Due to the low ratio between the number of trials and the number of examined features, channels were analyzed individually. The rationale for the single-channel analysis was to obtain good generalization for the classifier and to avoid overfitting (to prevent the classifier from “simply” memorizing the data).

Four binary classification problems were addressed: 1) contralateral thumb versus contralateral index finger, 2) ipsilateral thumb versus ipsilateral index finger, 3) contralateral thumb versus ipsilateral thumb, and 4) contralateral index finger versus ipsilateral index finger.

For each time interval, the DSLVQ method was repeated 100 times (DSLVQ parameter setup: 3 codebooks per class, 2000 training iterations). Random subsampling was used to assess the capability of the classifier to generalize to an independent data set. For each DSLVQ run, a randomly selected 50% subset of the data was used to train the classifier and to identify relevant features. The remaining 50% was used to test the classifier's performance.

## Results

### Time-Frequency Maps

The computed time-frequency maps were projected onto a template brain based on the postoperative skull radiograph.<sup>20</sup> These maps show widespread movement-related patterns in lower frequency ranges (6–40 Hz) and spatially more focused changes in higher frequency ranges (> 50 Hz). Figure 2 shows examples of these power modulations over selected sensorimotor hand areas. The maps furthermore show that contralateral and ipsilateral changes overlap to a large degree. Ipsilateral movements, however, induce less pronounced activity, particularly in the higher frequency ranges, than do contralateral movements.

### Single-Trial Classification

The results of the DSLVQ analysis are summarized in Fig. 3. Most discriminative electrodes were found over sensorimotor hand areas and were topographically focused. The topographic focus was more pronounced for contralateral movements, as ipsilateral movement classification occurred over a more widespread distribution.

For each classification task, Fig. 3 shows the computed classification performance, the contribution of the analyzed spectral components to correct classification



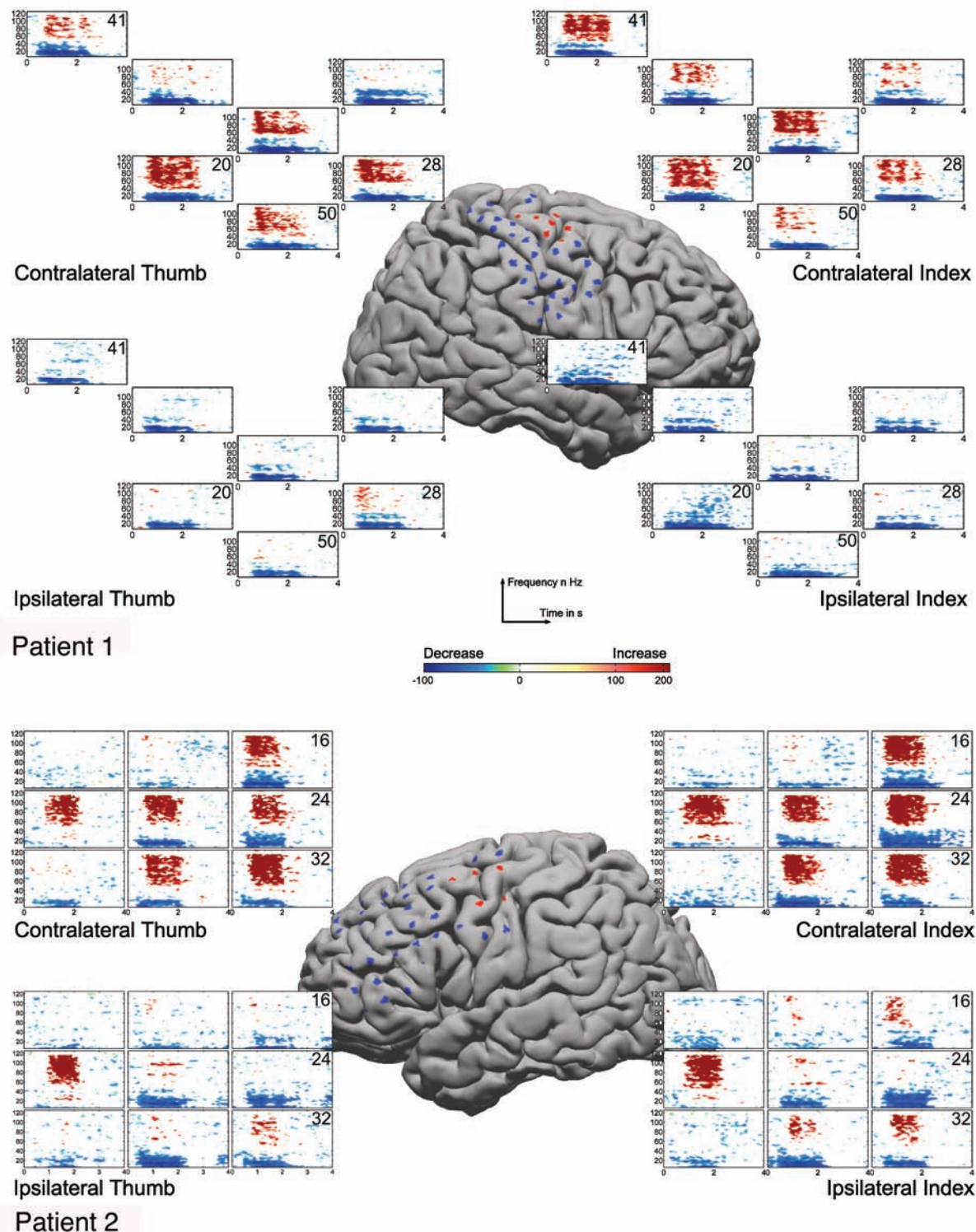


Fig. 2. Time-frequency maps for contralateral and ipsilateral thumb and index finger movements for both subjects. Electrode positions are marked on the template brain. Significant ( $\alpha = 0.01$ ) power modulations for highlighted (red) electrodes are topographically arranged for each motor task. Time  $t = 0$  seconds represents the time of cue onset. Each plot shows a 4-second period after cue onset. The frequency range is 8–125 Hz. The numbers in the right upper corner of some maps are the numbers of the electrodes and indicate the electrode relevant for classification.

TABLE 1: Distinction-sensitive LVQ classification performance\*

Pt No.	Classification	Ch	All (mean $\pm$ SD)	Selected Feature Subsets		
				Components†	Mean $\pm$ SD	Std Mean $\pm$ SD
1	contralat thumb vs contralat index	41	81.7 $\pm$ 7.3	65–90, 90–105, 105–120	<b>90.0</b> $\pm$ 5.0	73.4 $\pm$ 7.8
	ipsilat thumb vs ipsilat index	28	<b>66.6</b> $\pm$ 7.1	20–30, 95–105	65.7 $\pm$ 8.9	58.9 $\pm$ 6.9
	contralat thumb vs ipsilat thumb	50	<b>94.7</b> $\pm$ 3.3	60–100	93.9 $\pm$ 5.4	88.8 $\pm$ 5.5
	contralat index vs ipsilat index	20	<b>98.5</b> $\pm$ 1.5	36–60	96.4 $\pm$ 2.2	91.3 $\pm$ 4.6
2	contralat thumb vs contralat index	16	79.2 $\pm$ 6.9	80–115	<b>83.6</b> $\pm$ 6.2	75.9 $\pm$ <b>7.8</b>
	ipsilat thumb vs ipsilat index	16	81.3 $\pm$ 5.3	12–16, 70–95	<b>81.5</b> $\pm$ 6.4	77.8 $\pm$ 7.3
	contralat thumb vs ipsilat thumb	32	100.0 $\pm$ 0.0	70–115	<b>100.0</b> $\pm$ 0.0	100 $\pm$ 0.3
	contralat index vs ipsilat index	24	100.0 $\pm$ 0.0	80–115	<b>100.0</b> $\pm$ 0.0	99.9 $\pm$ 5.7
Average			87.8		<b>88.9</b>	83.3

\* The best performing individual channel and the mean ( $\pm$  SD) classification accuracy (%) for all features, for selected feature subsets, and for the standard frequency ranges 8–30 Hz and 76–100 Hz are summarized for each subject and classification task. *Bold values* indicate the maximum accuracy for each classification task. Abbreviations: Ch = channel; Pt = patient; Std = standard frequency ranges.

† The identified most discriminant frequency components.

(feature relevance) and the averaged movement pattern for each finger. The reported classification accuracies are the average values over the 100 random subsampling DSLVQ runs. An average classification accuracy (average of the maximum accuracy for each classification task) of 87.8% was achieved. To judge the computed classification performance, a comparison with random classification was performed. With 2 classes, 30 trials per class, and the same probability of occurrence for each trial ( $p = 0.5$ ), the upper level of chance classification at  $\alpha = 0.01$  (0.05) is 72.1 (66.9)%.<sup>23</sup> Except for the comparison in Patient 1 of ipsilateral thumb versus ipsilateral index, all classification accuracies were significantly better than random.

To investigate the computed feature relevance, the DSLVQ method was applied to selected feature subsets and to lower (8–30 Hz) and higher (76–100 Hz) frequency ranges.<sup>40</sup> The DSLVQ algorithm was applied as described in *Methods (Feature Selection and Single Trial-Classification)*. Table 1 summarizes the most discriminative frequency components derived from the DSLVQ feature relevance estimation (Fig. 3) and the computed classification accuracies. Reducing the dimensionality of the feature—that is, reducing features that do not contribute to correct classification—increases the average accuracy by 1.1% (from 87.8 to 88.9%). Two-tailed t-tests between the computed classification accuracies show that the selected subsets perform equally or significantly better (Table 2). The average accuracy for the standard frequency bands was 83.3%. Except for the 2 cases of perfect classification for Patient 2, the identified feature subsets performed significantly better than the standard frequency ranges.

## Discussion

The time-frequency maps show similar patterns in both patients during execution of movement (Fig. 2): focal broadband power increases in higher frequencies (> 50 Hz) and a widespread power decrease in lower frequencies (8–40 Hz). These findings are in accordance with

previous findings in the literature.<sup>4,5,19,22,24</sup> Additionally the maps suggest that similar activation patterns are induced during both contralateral and ipsilateral movements. The ipsilateral movement-related power modulations are not as prominent as the contralateral ones. However, high-frequency modulations during ipsilateral movement appear to be even more focal than those during contralateral movement.

In agreement with these characteristic patterns, the results of the single-trial DSLVQ analysis confirm that electrodes placed over sensorimotor hand areas are most relevant for the classification between the different finger movement tasks. Electrodes with the most prominent power modulations were usually selected by the DSLVQ method. Expectedly the average classification accuracies increase during finger motion and fall below chance level after movement stops. The accuracies reported in Table 1 suggest that a very general subdivision of the frequency range into lower (8–30 Hz) and higher (76–100 Hz) frequency ranges provides enough information to discriminate significantly better than chance between the different finger movements. Optimizing the frequency components, however, increases the average classification performance by 5.6% (Table 1, from 83.3 to 88.9%). The benefit of an accurate selection is most obvious for the classification of contralateral thumb versus contralateral index finger for Patient 1. The found subdivision of the higher frequency range into 3 smaller sub-bands boosts the accuracy from 73.8% for standard bands to 89.7%. This suggests that from a machine learning point of view, it is meaningful to investigate the finer structure of the higher frequency band and to isolate further such narrow-band activities.

It is interesting to note that the comparison of the power modulation maps for ipsilateral thumb and ipsilateral index finger movements for Patient 1 showed a significant increase in the power of higher frequencies over Electrode 28. The DSLVQ analysis found the highest classification performance for the same electrode. The single-trial performance, however, was at chance level.



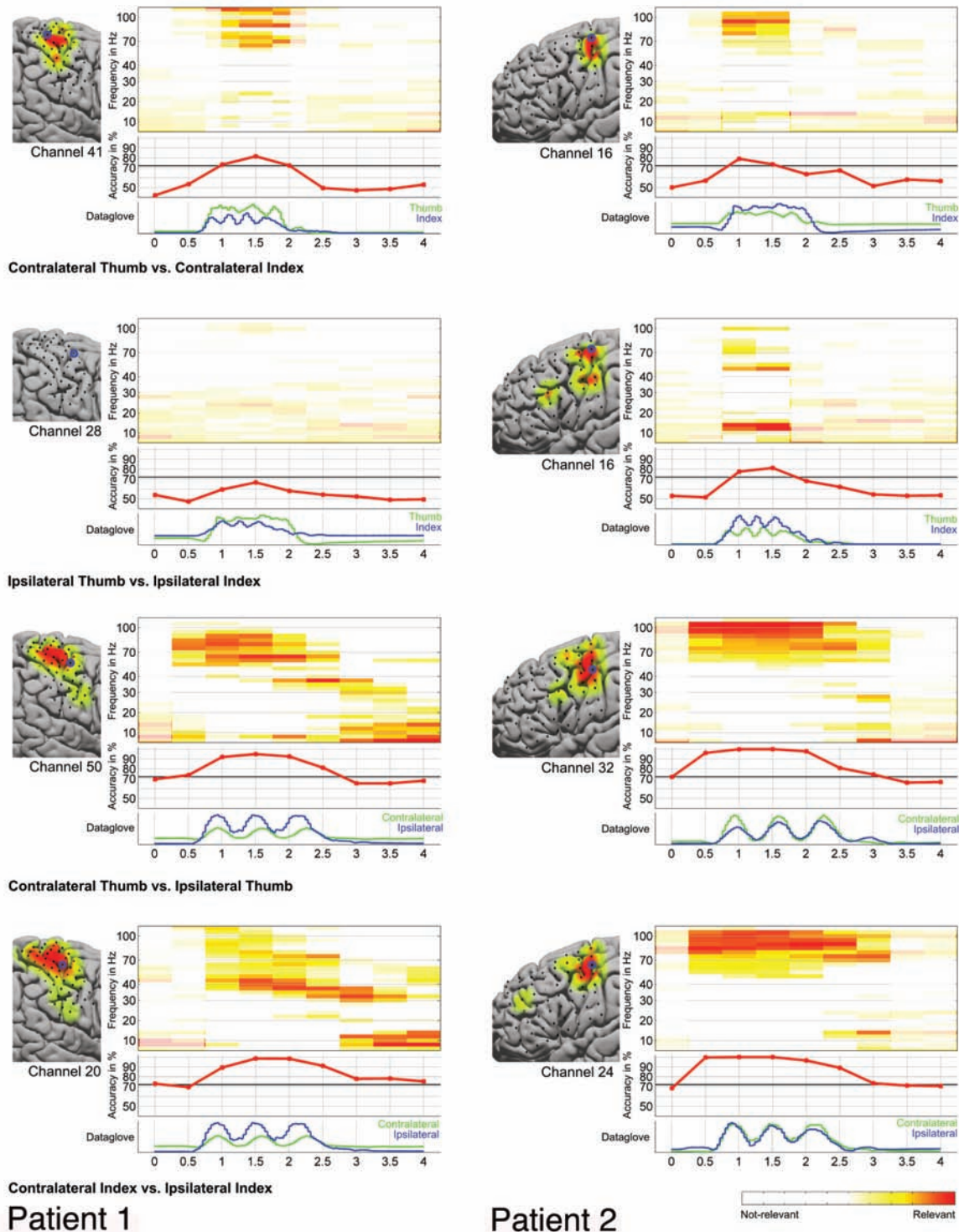


FIG. 3. Distinction-sensitive LVQ single-trial classification results. The template brain shows areas where the classification accuracy was better than random ( $> 72.1\%$ ). The most discriminative electrode for each classification task is marked with a *blue circle*. The plots and curves on the right-hand side show the most relevant spectral components (*upper plot*), the DSLVQ classification accuracies for all spectral components (*middle plot*), and the average digit movements recorded with the data glove (*lower plot*). The dashed lines in the accuracy plots show the level of random classification. The DSLVQ feature relevance estimation is only meaningful if the classification performance is better than random. Components that are not reliable are only faintly indicated.

**TABLE 2: Comparison of classification performance for all features versus selected subsets and for the standard frequency ranges versus the selected subsets\***

Classification	All vs Sel			Std vs Sel	
	t	df	p Value	t	df
contralat thumb vs contralat index	-9.847	99	0.000†	16.499	99
ipsilat thumb vs ipsilat index	0.881	99	0.380	6.195	99
contralat thumb vs ipsilat thumb	1.762	99	0.081	6.857	99
contralat index vs ipsilat index	8.385	99	0.000†	10.313	99
contralat thumb vs contralat index	-4.994	99	0.000†	7.452	99
ipsilat thumb vs ipsilat index	-0.245	99	0.807	3.607	99
contralat thumb vs ipsilat thumb				1.000	99
contralat index vs ipsilat index				1.750	99

\* Sel = selected feature subsets.

† Statistically significant by 2-tailed t-test ( $\alpha = 0.01$ ).

One can expect an improvement in classification accuracy by combining features from different electrodes or by incorporating the temporal structure of these power modulations at different frequencies. In this study, due to the reduced number of trials, we only considered the average spectral power over a 1-second time interval extracted from individual electrodes.

To explore the discriminative power of the identified channels (Table 1), a 4-class DSLVQ analysis was computed for each patient. Parameters as described earlier in the paper were used. To limit the number of features for each patient, only channels listed in Table 1 were included. By selecting just 3 and 5 features for Patients 1 and 2, respectively, maximum accuracies of 74.8 and 83.1% were calculated. Note that the theoretical chance

level for a 4-class problem, where each class has the same number of occurrences, is 25%. Figure 4 shows the classification accuracy curves and the distribution of the 3 selected band power features for Patient 2. The distribution plots suggest that contralateral movements induced higher power increases than did ipsilateral motion. Such a distribution was also visible for Patient 1 and is the reason for the high classification accuracies between ipsilateral and contralateral finger movements for the same digit (see also Table 1 and Fig. 3). Differences between different fingers of the same hand were much less pronounced, resulting in a lower discriminative power.

Patient 1 had a somewhat atypical electrode array in that the resolution was 30% better than that of our prior electrode arrays (7-mm interelectrode distance). It is of

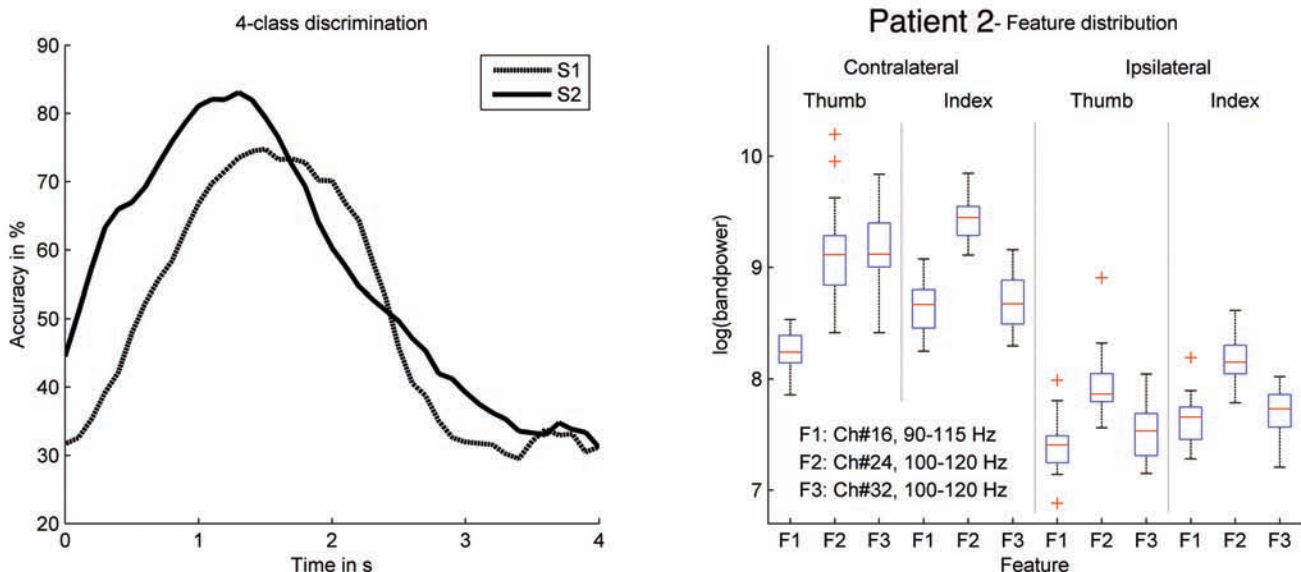


FIG. 4. *Left:* Line graph showing the average 4-class classification accuracy over time for both patients. *Right:* Box and whisker plots summarizing the distribution of the 3 most discriminative selected features (F1, F2, and F3) for Patient 2. The boxes have lines at the lower quartile, median, and upper quartile values. The whiskers are lines extending from each end of the boxes to show the extent of the rest of the data. Outliers are data with values beyond the ends of the whiskers. s = seconds; S1 = Patient 1; S2 = Patient 2.

interest that we achieved greater discriminative ability in this case than with the 1-cm interelectrode array. The existence of microstructure within the ECoG signal has previously been demonstrated for seizures<sup>34,39</sup> and for speech function.<sup>1</sup> Our results suggest that higher spatial resolution of electrode arrays may pave the way for classification of increasingly fine and complex movements from ECoG signals.

### Conclusions

In this article, we provided further evidence for the utility of ECoG in brain-computer interfacing by demonstrating that individual finger movements from both the ipsi- and contralateral hands can be discriminated from ECoG signals. We found that time-frequency patterns over sensorimotor areas for contralateral and ipsilateral movements overlap to a large degree. Ipsilateral movements, however, result in less pronounced activity compared with contralateral movements, especially in the case of power increases.

By using the full set of frequencies present in the ECoG signal, we obtained classification accuracy superior to that obtained with previous methods that look a priori at an isolated band of frequencies.<sup>18,33</sup> Our results also suggest that single-trial classification can be improved by selecting patient-specific frequency components in higher frequency bands (> 50 Hz). This is consistent with the idea that only coadaptation of brain and machine allows the most accurate and robust direct brain-computer interaction in a limited amount of time.

Finally, our discovery that ipsilateral hand movements can be discriminated from ECoG is particularly exciting for BCI applications, because after unilateral damage to one hemisphere, brain signals from the intact hemisphere could potentially be used to regain control of ipsilateral movement through muscle or nerve stimulation.

### Disclaimer

The authors report no conflict of interest concerning the materials or methods used in this study or the findings specified in this paper.

### References

1. Blakely T, Miller KJ, Rao RPN, Holmes MD, Ojemann JG: Localization and classification of phonemes using high spatial resolution ECoG grids. **Conf Proc IEEE Eng Med Biol Soc** 1:4964–4967, 2008
2. Bland M: **An Introduction to Medical Statistics**, ed 2. Oxford: Oxford Medical Publications, 2000
3. Blankertz B, Dornhege G, Krauledat M, Mueller K-R, Kunzmann V, Losch F, et al: The Berlin brain-computer interface: EEG-based communication without subject training. **IEEE Trans Neural Syst Rehabil Eng** 14:147–152, 2006
4. Crone NE, Miglioretti DL, Gordon B, Lesser RP: Functional mapping of human sensorimotor cortex with electrocorticographic spectral analysis. II. Event-related desynchronization in the gamma band. **Brain** 121:2301–2315, 1998
5. Crone NE, Miglioretti DL, Gordon B, Sieracki JM, Wilson MT, Uematsu S, et al: Functional mapping of human sensorimotor cortex with electrocorticographic spectral analysis. I. Alpha and beta event-related desynchronization. **Brain** 121:2271–2299, 1998
6. Dat TH, Shue L, Guan C: Electrocorticographic signal classification based on time-frequency decomposition and nonparametric statistical modeling. **Conf Proc IEEE Eng Med Biol Soc** 1:2292–2295, 2006
7. Donoghue JP: Bridging the brain to the world: a perspective on neural interface systems. **Neuron** 60:511–521, 2008
8. Felton EA, Wilson JA, Williams JC, Garell PC: Electrocorticographically controlled brain-computer interfaces using motor and sensory imagery in patients with temporary subdural electrode implants. Report of four cases. **J Neurosurg** 106:495–500, 2007
9. Graitmann B, Huggins J, Levine S, Pfurtscheller G: Towards a direct brain interface based on human subdural recordings and wavelet packet analysis. **IEEE Trans Biomed Eng** 51:954–962, 2004
10. Graitmann B, Huggins JE, Levine SP, Pfurtscheller G: Visualization of significant ERD/ERS patterns in multichannel EEG and ECoG data. **Clin Neurophysiol** 113:43–47, 2002
11. Graitmann B, Huggins JE, Schlogl A, Levine SP, Pfurtscheller G: Detection of movement-related desynchronization patterns in ongoing single-channel electrocorticogram. **IEEE Trans Neural Syst Rehabil Eng** 11:276–281, 2003
12. Graitmann B, Pfurtscheller G: Quantification and visualization of event-related changes in oscillatory brain activity in the time-frequency domain. **Prog Brain Res** 159:79–97, 2006
13. Hill NJ, Lal TN, Schröder M, Hinterberger T, Wilhelm B, Nijboer F, et al: Classifying EEG and ECoG signals without subject training for fast BCI implementation: comparison of non-paralyzed and completely paralyzed subjects. **IEEE Trans Neural Syst Rehabil Eng** 14:183–186, 2006
14. Hinterberger T, Widman G, Lal TN, Hill J, Tangermann M, Rosenstiel W, et al: Voluntary brain regulation and communication with electrocorticogram signals. **Epilepsy Behav** 13:300–306, 2008
15. Hochberg LR, Serruya MD, Friehs GM, Mukand JA, Saleh M, Caplan AH, et al: Neuronal ensemble control of prosthetic devices by a human with tetraplegia. **Nature** 442:164–171, 2006
16. Leuthardt EC, Miller KJ, Schalk G, Rao RPN, Ojemann JG: Electrocorticography-based brain computer interface—the Seattle experience. **IEEE Trans Neural Syst Rehabil Eng** 14:194–198, 2006
17. Leuthardt EC, Schalk G, Moran DW, Ojemann JG: The emerging world of motor neuroprosthetics: a neurosurgical perspective. **Neurosurgery** 59:1–14, 2006
18. Leuthardt EC, Schalk G, Wolpaw JR, Ojemann JG, Moran DW: A brain-computer interface using electrocorticographic signals in humans. **J Neural Eng** 1:63–71, 2004
19. Miller KJ, Leuthardt EC, Schalk G, Rao RPN, Anderson NR, Moran DW, et al: Spectral changes in cortical surface potentials during motor movement. **J Neurosci** 27:2424–2432, 2007
20. Miller KJ, Rao RJ, den Nijs M, Makeig S, Hebb AO, Ojemann JG: Cortical surface localization from x-ray and simple mapping for electrocorticographic research: the “Location On Cortex” (LOC) package for MATLAB. **J Neurosci Methods** 162:303–308, 2007
21. Miller KJ, Shenoy P, den Nijs M, Sorensen LB, Rao RPN, Ojemann JG: Beyond the gamma band: the role of high frequency features in movement classification. **IEEE Trans Biomed Eng** 55:1634–1637, 2008
22. Miller KJ, Zanos S, Fetz EE, den Nijs M, Ojemann JG: Decoupling the cortical power spectrum reveals individual finger representation in humans. **J Neurosci** 29:3132–3137, 2009
23. Müller-Putz GR, Scherer R, Brunner C, Leeb R, Pfurtscheller G: Better than random? A closer look on BCI results. **Int J Bioelectromagnetism** 10:52–55, 2008
24. Pfurtscheller G, da Silva FHL: Event-related EEG/MEG



## Finger movements for electrocorticographic BCIs

- synchronization and desynchronization: basic principles. **Clin Neurophysiol** **110**:1842–1857, 1999
25. Pistohl T, Ball T, Schulze-Bonhage A, Aertsen A, Mehring C: Prediction of arm movement trajectories from ECoG-recordings in humans. **J Neurosci Methods** **167**:105–114, 2008
26. Pregenzer M, Pfurtscheller G, Flotzinger D: Selection of electrode positions for an EEG-based brain computer interface (BCI). **Biomed Tech (Berl)** **39**:264–269, 1994
27. Ramsey NF, van de Heuvel MP, Kho KH, Leijten FS: Towards human BCI applications based on cognitive brain systems: an investigation of neural signals recorded from the dorsolateral prefrontal cortex. **IEEE Trans Neural Syst Rehabil Eng** **14**: 214–217, 2006
28. Schalk G, Kubanek J, Miller KJ, Anderson N, Leuthardt EC, Ojemann JG, et al: Decoding two-dimensional movement trajectories using electrocorticographic signals in humans. **J Neural Eng** **4**:264–275, 2007
29. Schalk G, McFarland DJ, Hinterberger T, Birbaumer N, Wolpaw JR: BCI2000: a general-purpose brain-computer interface (BCI) system. **IEEE Trans Biomed Eng** **51**:1034–1043, 2004
30. Schalk G, Miller KJ, Anderson NR, Wilson JA, Ojemann JG, Moran DW, et al: Two-dimensional movement control using electrocorticographic signals in humans. **J Neural Eng** **5**:75–84, 2008
31. Scherer R, Graimann B, Huggins JE, Levine SP, Pfurtscheller G: Frequency component selection for an ECoG-based brain-computer interface. **Biomed Tech (Berl)** **48**:31–36, 2003
32. Scherer R, Mohapp A, Grieshofer P, Pfurtscheller G, Neuper C: Sensorimotor EEG patterns during motor imagery in hemiparetic stroke patients. **Int J Bioelectromagnetism** **9**:155–162, 2007
33. Shenoy P, Miller KJ, Ojemann JG, Rao RPN: Generalizable features for electrocorticographic BCIs. **IEEE Trans Biomed Eng** **55**:273–280, 2008
34. Waziri A, Schevon CA, Cappell J, Emerson RG, McKhann GM II, Goodman RR: Initial surgical experience with a dense cortical microarray in epileptic patients undergoing craniotomy for subdural electrode implantation. **Neurosurgery** **64**:540–545, 2009
35. Wei Q, Gao X, Gao S: Feature extraction and subset selection for classifying single-trial ECoG during motor imagery. **Conf Proc IEEE Eng Med Biol Soc** **1**:1589–1592, 2006
36. Wei Q, Tu W: Channel selection by genetic algorithms for classifying single-trial ECoG during motor imagery. **Conf Proc IEEE Eng Med Biol Soc** **1**:624–627, 2008
37. Wisneski KJ, Anderson N, Schalk G, Smyth M, Moran D, Leuthardt EC: Unique cortical physiology associated with ipsilateral hand movements and neuroprosthetic implications. **Stroke** **39**:3351–3359, 2008
38. Wolpaw JR, McFarland D: Control of a two-dimensional movement signal by a noninvasive brain-computer interface in humans. **Proc Natl Acad Sci U S A** **101**:17849–17854, 2004
39. Worrell GA, Gardner AB, Stead SM, Hu S, Goerss S, Cascino GJ, et al: High-frequency oscillations in human temporal lobe: simultaneous microwire and clinical macroelectrode recordings. **Brain** **131**:928–937, 2008
40. Zanos S, Miller KJ, Ojemann JG: Electrocorticographic spectral changes associated with ipsilateral individual finger and whole hand movement. **Conf Proc IEEE Eng Med Biol Soc** **1**:5939–5942, 2008

---

Manuscript submitted March 15, 2009.

Accepted April 30, 2009.

*Address correspondence to:* Jeffrey G. Ojemann, M.D., Seattle Children's Hospital, University of Washington, Seattle, Washington 98105. email: jojemann@u.washington.edu.